Superconductor
Science and
Technology

PAPER • OPEN ACCESS

Control of turn-to-turn contact resistivity in no-insulation REBCO coils

To cite this article: Jun Lu *et al* 2026 *Supercond. Sci. Technol.* **39** 075034

IOP Publishing Supercond. Sci. Technol. **39** (2026) 075034 https://doi.org/10.1088/1361-6668/ae8b32

Superconductor Science and Technology

OPEN ACCESS

RECEIVED
14 April 2026

REVISED
24 June 2026

ACCEPTED FOR PUBLICATION
15 July 2026

PUBLISHED
28 July 2026

PAPER

Control of turn-to-turn contact resistivity in no-insulation REBCO coils

Jun Lu*, Kwangmin Kim, Iain Dixon, Justin Deterding, Emsley Marks, Brent Jarvis, Denis Markiewicz, Hongyu Bai and Mark Bird

National High Magnetic Field Laboratory, Tallahassee 32310, FL, United States of America
* Author to whom any correspondence should be addressed.

E-mail: junlu@magnet.fsu.edu

Keywords: REBCO, no-insulation, contact resistance, superconducting magnet

Abstract

No-insulation (NI) REBCO magnets with optimized contact resistivity feature short ramp times and low ramp losses while maintaining the advantages of NI coils with high engineering current density and tolerance for defects in the REBCO conductor. Control of the turn-to-turn contact resistivity (ρ_c) is key to NI technology. ρ_c must be sufficiently high to prevent a large transient current, which could result in high mechanical stress during magnet quenches. Meanwhile it must be lower than the quench propagation limit to avoid conductor burn-out during a quench. Therefore, it is critical to control ρ_c within a suitable range of values which is usually coil specific. Previously, we discovered that ρ_c between two REBCO tapes with a stainless steel interlayer decreases dramatically with contact pressure cycling by up to three orders of magnitude. This drastic change makes it impossible to design a suitable ρ_c value for a stainless steel co-wound NI magnet. In this work, we first present methods for mitigating ρ_c pressure cycling sensitivity. We found that by adding conductive fillers, such as conductive paste or epoxy, the ρ_c load cycling sensitivity is largely mitigated. For dry-wound coils, ρ_c load cycling sensitivity is mitigated by coating REBCO tape with a layer of 2–3 μm of PbSn solder. In addition, ρ_c can be controlled by oxidizing the stainless steel co-wind tape by heating stainless steel tapes at different temperatures in air. Using above methods, short sample tests showed that ρ_c was controlled to prescribed values of 1000 and 5000 $\mu\Omega$-cm^2 and was not sensitive to contact pressure cycling up to 30 000 cycles at 4.2 K. The new ρ_c control method was applied to a 6 double-pancake test coil which was tested at 4.2 K. The ρ_c in this test coil was comparable with the short sample results. This demonstrated the ability of this new method to control ρ_c in large coils. Moreover, we propose a method of measuring coil's ρ_c by the decay time of coil's inductive voltage.

1. Introduction

No-insulation (NI) REBCO magnet technologies allow for a high engineering current density compared with their conventional insulated counterparts. They have been developing rapidly over the past 15 years. Using NI technology, an extremely high field of 45.2 T has been achieved in a background field of 31 T [1]. In addition, fields over 30 T have been achieved by NI REBCO insert coils in the background field provided by either superconducting [2–4] or resistive magnets [5]. The key to NI technology is the control of turn-to-turn contact resistivity (ρ_c). A low ρ_c in NI magnets results in long charging delays and high ac losses during field ramps, which are undesirable for a user magnet that requires frequent field ramps. In addition, during a magnet quench low ρ_c results in large transient current in both radial and azimuthal directions [4, 6] which in turn causes high mechanical stresses that may be difficult to mitigate. On the other hand, a high ρ_c compromises the advantage of stability and quench self-protection ability and risks burn-outs at hotspots in the magnet. For these reasons, there have been many studies on ρ_c measurements and control in recent literature. The studies on ρ_c measurements of short samples

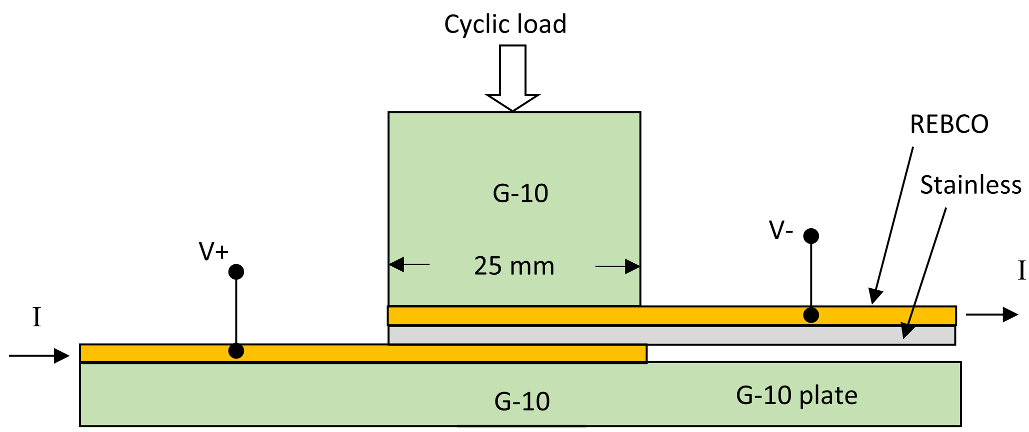

Figure 1. Schematic of contact resistance test device. The device was placed in a universal test machine, and tests were performed in liquid helium or liquid nitrogen bath.

can be found in [7–9]. Measurements of ρ_c in REBCO coils are published in [10, 11]. In the afore mentioned NI magnets that reached 30 T and above, none of them had conductor or co-wind surface engineered to achieve a prescribed ρ_c. To develop methods to control ρ_c, several groups have achieved various levels of success [12–14]. However, a reliable control method that can engineer a prescribed ρ_c value in a wide range and is proved in large NI coil tests is still lacking.

Since high-field REBCO magnets are often stress-limited, co-wound stainless steel tapes are often used for mechanical reinforcement [15, 16]. This allows, in principle, to implement NI techniques by controlling the contact resistance between REBCO and co-wind tape. For this reason, the contact resistance of interface between REBCO and stainless steel was studied [7]. We discovered however, that contact pressure cycling at 4.2 K dramatically reduces ρ_c [7]. This considerable ρ_c variation during the lifetime of a magnet makes control of ρ_c practically impossible.

In this study, we developed a method to mitigate the load cycling sensitivity of ρ_c by coating REBCO coated conductor with eutectic PbSn solder. Subsequently, the control of ρ_c was achieved by surface oxidation of the stainless steel co-wind tape at different temperatures. This combination of methods was successfully used in a 6 double-pancake test coil named PTC-6. The details of the development of this combined method are described, and data from PTC-6 tests will be presented. As a part of PTC-6 coil testing, a new method of measuring coil ρ_c was proposed and demonstrated.

2. Experiment

REBCO tapes were SCS4050-AP by SuperPower Inc. They were 4 mm wide with 50 μm thick Hastelloy C-276 substrate and 20 μm Cu stabilizer on each side. The stainless steel co-wind were 316L half hard tapes that were 4 mm wide and 25 μm thick, procured from Ulbrich of Illinois, Inc.

ρ_c tests using short samples were performed at 77 and 4.2 K in a device as shown in figure 1 [17]. A REBCO/stainless steel/REBCO stack with a 25 mm long overlap was put under load in tape thickness direction in liquid nitrogen or liquid helium bath. The load was cycled between 250 and 2500 N (corresponds to 2.5–25 MPa contact pressure) at 5 Hz by a hydraulic universal test machine (MTS corporation). The contact resistance was measured by a 4-probe method with a current of 1 A.

A key step in this work was mitigation of load cycling sensitivity by coating a layer of relatively soft material on REBCO tapes. For this, we developed a reel-to-reel solder coating machine, a schematic of which is shown in figure 2. The as-received REBCO tape went through a molten eutectic PbSn solder pot at 240 °C. The excessive molten solder on REBCO tape was then wiped by a pair of silicone pads as soon as it came out of the solder pot. In this process, the typical linear speed of REBCO tape was 6 m min^{-1}. The resultant coating thickness was about 2–3 μm as measured by cross-sectional microscopy. The effect of the coating process on REBCO properties was checked by measuring 77 K self-field Ic and RRR of the copper stabilizer before and after coating. No degradation was observed within the measurement error.

We control ρ_c via surface treatment of the stainless steel co-wind tape. One method was oxidizing it in air in a vertical furnace. We adjust the furnace temperature to control the degree of oxidation, which

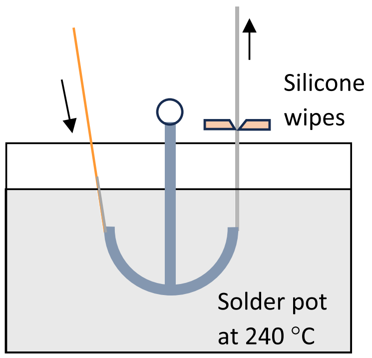

Figure 2. Schematic of the solder coating process. REBCO tape slid through the half-circle fixture in the solder pot. The half-circle fixture has a radius of 40 mm. The solder was eutectic PbSn. The linear speed was 6 m min^{-1}.

Table 1. ρ_c control methods used in this work.

Treatment	Method	Description	Intended effect
Stainless steel surface	Thermal oxidation	300–600 C in air	Increase ρ_c
	Chemical oxidation	Ultra-Black® 407 l	Increase ρ_c
	Coating of SS	TiN, Al_2O_3 by atomic layer deposition	Increase ρ_c
REBCO surface	Solder coating	Reel-to-reel hot dip coating $Pb_{37}Sn_{63}$	Decrease ρ_c
Interface	Silver epoxy	Apply to interface and cured under 25 MPa pressure	Decrease ρ_c and/or mitigate load cycling sensitivity
	Silver paste		
	Stycast 1266		
	Paraffin	Vacuum impregnation at 25 MPa	

Table 2. Parameters of PTC-6 test coil.

Parameters	PTC-6
Number of double-pancakes	6
Inner winding radius a_1 (mm)	22
Outer winding radius a_2 (mm)	40
Outer radius of overband a_3 (mm)	42
Number of turns per disk	123
I_{max} (A)	240
$B_{z\text{-}max}$ (T)	11.3
Inductance (mH)	82.78
Winding stress (MPa)	35
Targeted ρ_c ($\mu\Omega$-cm^2)	1000

in turn controls ρ_c. The linear speed of this reel-to-reel process was 1 m min^{-1}. Additional methods of oxidation were also explored. For instance, we immersed stainless steel samples in a solution of Ultra-Blak®407 l (Electrochemical Products, Inc.), which contains 60–68 wt% NaOH, 10–20 wt% $NaNO_3$, and 0.05–0.15 wt% $K_2Cr_2O_7$ [18], at 120 °C for different times. We also experimented with coating the 600 atomic layers of TiN and Al_2O_3 by atomic layer deposition (ALD). Table 1 lists the ρ_c control methods experimented in this work.

To demonstrate the ρ_c control over a practical length, an NI test coil, named as PTC-6, was designed fabricated and tested. The coil parameters of PTC-6 are listed in table 2. The coil consists of 6 double-pancakes wound with solder-coated REBCO tapes and co-wound with surface treated stainless steel tapes. The parameters a_1, a_2, and a_3 are the inner, outer and overband radius respectively. The winding stress for both REBCO and stainless steel co-wind was 35 MPa. The targeted ρ_c was 1000 $\mu\Omega$-cm^2 decided based on coil quench considerations.

In general, the value of ρ_c for a coil is selected to suppress the peak currents that develop during quench transients, balanced on maintaining stability [6]. Since the contact area increases with coil size, the magnitude of ρ_c must also increase. Thus, the reason for developing a way to control ρ_c over a wide range, as is done in this study.

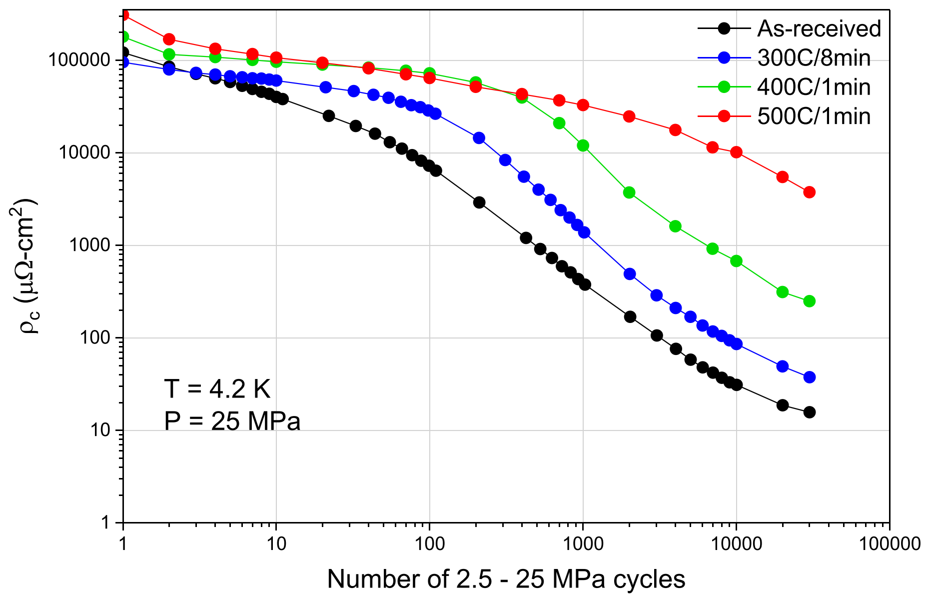

Figure 3. ρ_c of REBCO/stainless steel/REBCO stack with stainless steel tapes oxidized at various temperatures and times. Except for the as-received one, the stainless steel tapes were etched by 37% HCl for 5 min at room temperature to remove the native oxides before oxidation.

For improved stability and proper flow of radial current during quench, radial compression is necessary. The PTC-6 coil contains stainless steel tape for overbanding, as noted by the *a3* parameter in table 2, to increase the radial contact pressure. Radial contact pressure is dependent on radius and is zero at the inner radius and maximum at the REBCO winding to overbanding interface, *a2*. The maximum radial pressure for PTC-6 is 20 MPa.

The coil was tested at 4.2 K in a 6.5 T background field provided by a NbTi magnet. The average ρ_c was determined by decay time of the central field after a sudden discharge at 5 A or by decay time of the inductive voltage after a ramp-and-hold operation. The decay time constant was determined by the time for the signal to decay to 1 e $^{-1}$ of its original value. The average contact resistance R_c of the entire coil was calculated using a simple lumped circuit model,

$$R_c = L/\tau \tag{1}$$

where L is the coil's inductance which was calculated and confirmed by the inductive voltage value during a current ramp. Subsequently, the contact resistivity ρ_c was calculated by,

$$R_c = \sum_{i=1}^{N} \frac{\rho_c}{2\pi r_i w} = \frac{\rho_c}{2\pi w} \sum_{i=1}^{N} \frac{1}{r_i} \tag{2}$$

$$\rho_c = 2\pi w R_c / \sum_{i=1}^{N} \frac{1}{r_i} \tag{3}$$

where N is the total number of turns of all pancakes, and r_i the radius of ith turn, w the tape width.

3. Results

3.1. Preliminary development for ρc *control*

Control of ρ_c is the ability to adjust ρ_c to a specified value for NI magnet design. In case of REBCO/stainless steel contact, an obvious solution is to form a thin oxide layer on stainless steel with controlled thickness [7]. Figure 3 shows ρ_c of REBCO/stainless steel/REBCO stack at 4.2 K as a function of load cycle. REBCO tapes were in as-received condition, while the stainless steel tapes were oxidized in air at different temperatures for 1 min. ρ_c of the as received and lightly oxidized stainless steel were sensitive to load cycling due to the wear of the very thin oxide layer. After 30 000 cycles, ρ_c dropped up to 4 orders of magnitude. This makes effective ρ_c control practically impossible. The sensitivity

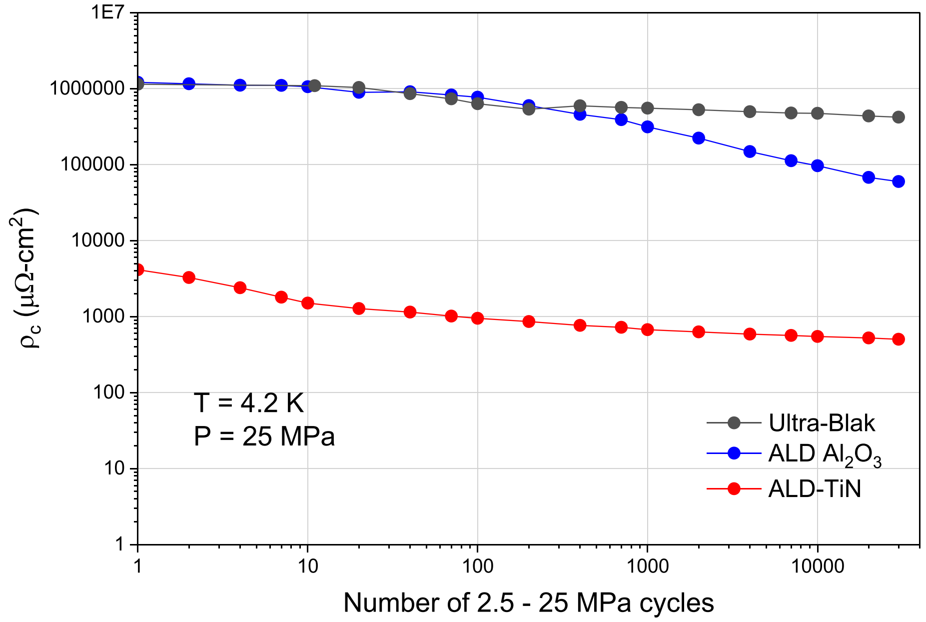

Figure 4. ρ_c vs. pressure cycles of 316 l stainless steel treated by Ultra-Blak 407 l, coated with TiN and Al_2O_3 by ALD.

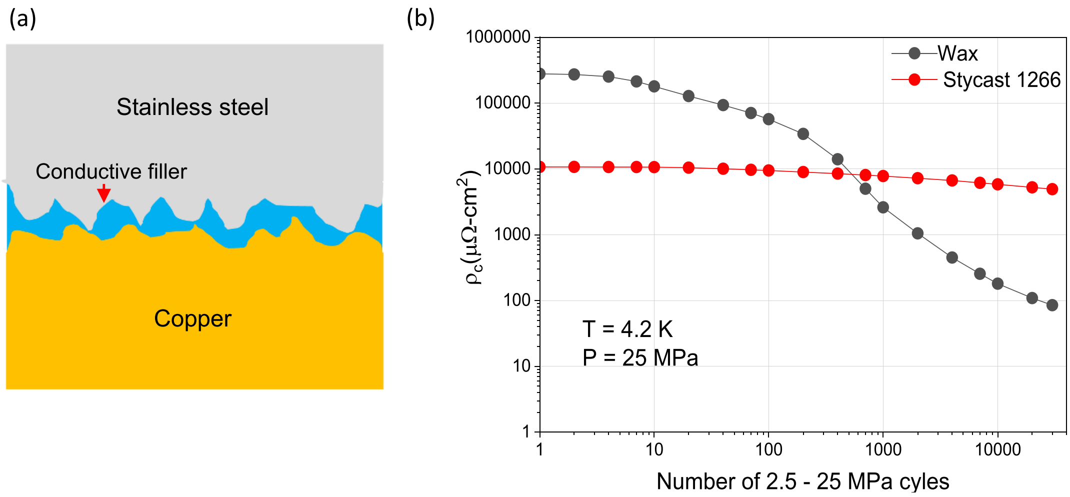

Figure 5. (a) Schematic of a contacting interface filled with impregnating material. (b) ρ_c of samples impregnated by paraffin wax and Stycast 1266 under 25 MPa contact pressure.

to load cycling decreased with increasing oxidation temperature within the range of 300 °C–500 °C. However, the ρ_c values were too high for our application and not very responsive to oxidation temperature. Therefore, the oxidation of stainless steel alone does not seem to be suitable for ρ_c control, and other methods of oxidation were experimented.

Figure 4 shows the results from stainless steel samples treated by Ultra-Blak for 15 min as well as the ones coated by TiN (300 layers) and Al_2O_3 (300 layers) by using ALD. With these useful developments, the sensitivity to load cycling was much reduced. However, ρ_c was still not very responsive to the change of process parameters, and scaling up these thin film growth techniques will be challenging. Additionally, it is difficult to obtain lower ρ_c values using Ultra-Blak alone.

The surfaces of the electroplated copper on REBCO and also the steel co-wind are not smooth as depicted in figure 5(a). The load cycling sensitivity is likely due to wear at the contact asperities where the localized stress is high. Therefore, if the local stress is distributed more evenly by filling the voids with a material at the contacting interface as depicted in figure 5(a), the wear and load cycling sensitivity would be reduced. We applied paraffin wax and Stycast 1266 epoxy fillers respectively between REBCO and stainless steel. The paraffin was impregnated in vacuum at about 100 °C under a 25 MPa contact pressure, while the Stycast 1266 was applied between REBCO and stainless steel and cured at ambient

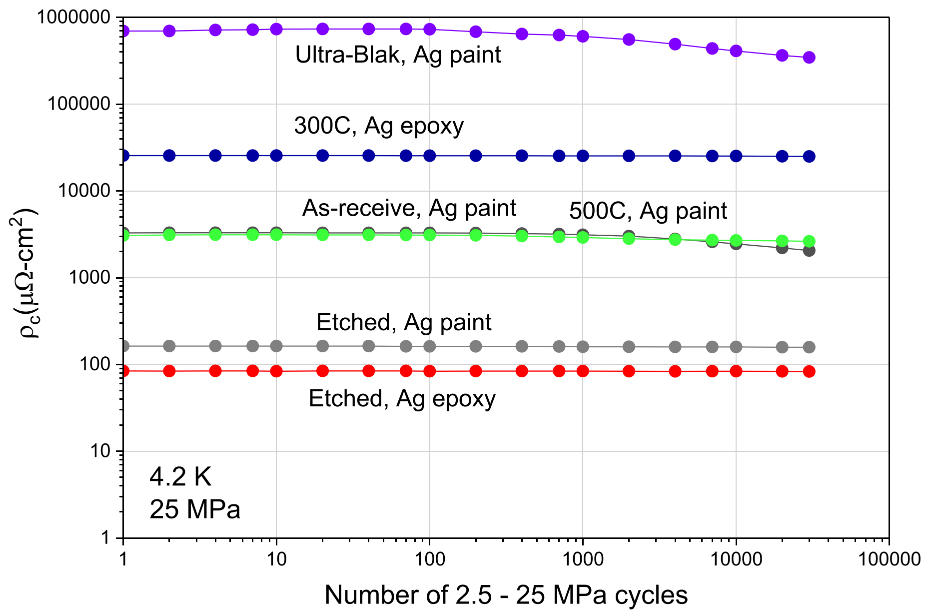

Figure 6. ρ_c versus load cycle for stacks of REBCO/stainless steel/REBCO where Ag paint (Dupont 4929 N) and silver epoxy (H20E, Epoxy Technology) were used as fillers at contact interfaces.

temperature under a 25 MPa contact pressure. Figure 5(b) shows their load cycling results. The initial ρ_c values are comparable with their dry contacts counterparts even though both paraffin and epoxy are insulating, which suggests that the contact asperities were free of impregnating materials. The sample impregnated with epoxy showed much improved cycling sensitivity as predicted. While the paraffin impregnated sample did not show improvement, as it is too weak to distribute the loads at the asperities and prevent wear of the oxide layer.

Encouraged by above results and with the goal of lowering ρ_c to a range that is responsive to thermal oxidation treatment, we applied conductive fillers between the contacting surfaces using silver paint (DuPont 4929 N) and silver epoxy (H20E by Epoxy Technology) respectively. The silver paint was cured in atmosphere for 16 h, the silver epoxy was cured at 135 C for 15 min, both under 25 MPa pressure. The results show much improved load cycling robustness as shown in figure 6. Meanwhile, the increase in the actual contact area by conductive fillers made ρ_c considerably lower. For instance, ρ_c with 500 °C oxidized stainless steel was 230 000 $\mu\Omega$-cm^2. With silver paint filler, ρ_c was only 3 000 $\mu\Omega$-cm^2, a factor of 70 reduction. This way, a wide range of ρ_c control can be achieved by changing temperature of thermal oxidation or using other oxidation methods as also shown in figure 6.

Another important experiment was to check the integrity of the oxide layers after a high transverse current in simulation of the radial current during a magnet quench. During a quench, the high radial transient current may irreversibly damage the oxide layer and change ρ_c. For this experiment, we used a capacitor bank to inject several 100 A current pulses across the 1 cm^2 contact at 4.2 K. Each pulse was several milliseconds long. For samples with ρ_c lower than 5000 $\mu\Omega$-cm^2, after such current injection, the effect was insignificant. For samples with higher ρ_c, reduction in ρ_c was observed to increase with initial ρ_c. This can be explained by localized burnout or dielectric breakdown of the oxide layer at the contact spots. Conceivably high initial ρ_c leads to higher voltage across the oxide layer and higher joule heating power; therefore, the oxide layer is more likely to be damaged. Figure 7 shows measured ρ_c reduction after several 100 A pulses as a function of initial ρ_c. It should be noted that the stainless steel samples used in this figure were treated with various methods.

To summarize this section, our preliminary research showed that the method of co-wind oxidation together with the use of a conductive filler seemed to allow for ρ_c control without load cycling sensitivity. It should be noted that similar approach was used by Bouloukakis [13] and more recently by Park *et al* [19] where copper and graphite filled conductive epoxy were used respectively, and filler composition was adjusted to control ρ_c. The shortcoming of this method, however, is that turn-to-turn bonding by epoxy may introduce thermal stress which could lead to severe Ic degradation [20]. Furthermore, in the wet winding process, the excessive conductive fillers could cause undesirable short circuits. All these

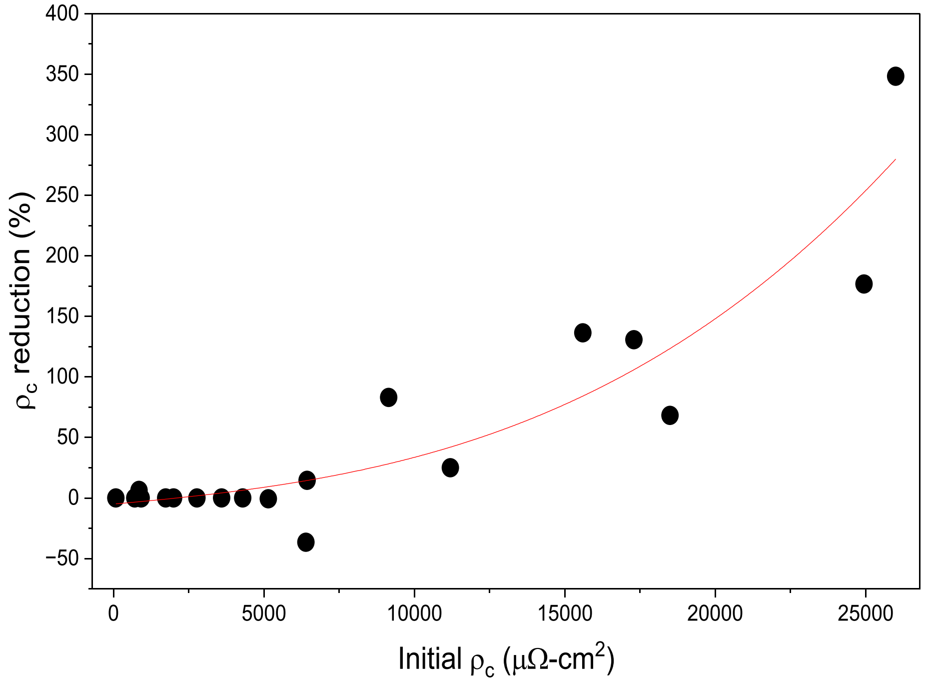

Figure 7. Correlation between initial ρ_c and reduction of ρ_c after several 100 A transverse current pulses. The stainless steel samples were treated by various methods. The solid line is a guide to the eye.

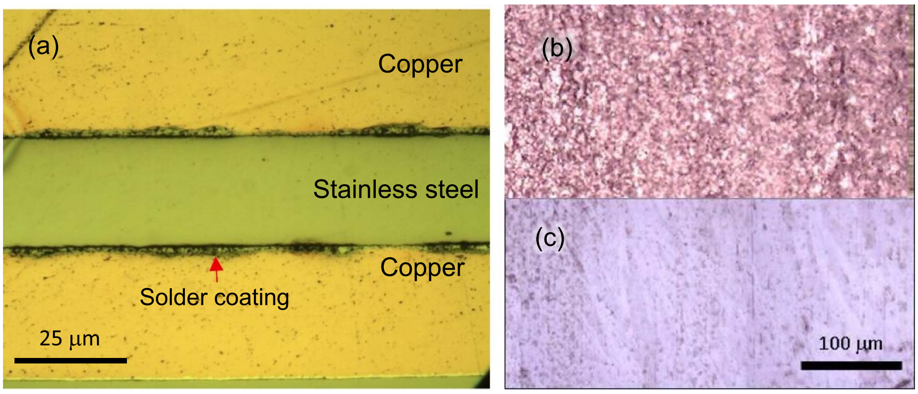

Figure 8. (a) a cross-sectional micrograph of REBCO/Stainless steel/REBCO interfaces. REBCO is coated with PbSn solder which seems to smooth out the relatively rough surface of Cu stabilizer of REBCO. (b) laser confocal microscopy of the as-received REBCO surface and (c) solder coated REBCO surface.

require significant development. Therefore, an alternative dry winding method was developed and will be described in the next section.

3.2. Control of ρ_c by solder coating REBCO and oxidation of the stainless steel

Since the load cycling effect was attributed to the wear of the very thin layer of oxides on stainless steel surface against copper stabilizer layer of the REBCO tape, an intuitive method of mitigation is to coat REBCO tape with a thin layer of material that is significantly softer than the electroplated copper layer. For instance, the eutectic PbSn solder has a hardness of only 16 Hv at room temperature [21], much softer than that of electroplated Cu of 180–220 Hv [22]. Although hardness at cryogenic temperatures for PbSn solder is not found in the literature, it is speculated to be significantly lower than that of copper. Therefore, it is conceivable that solder coated REBCO results in reduction in load cycling sensitivity.

Figure 8(a) shows a cross-section of a stainless steel tape between two solder-coated REBCO tapes. The average coating thickness was 2–3 μm which is sufficient to prevent copper from directly contacting the stainless steel. The surface morphology was characterized by laser confocal microscopy, and the comparison before and after solder coating is shown in figures 8(b) and (c). The coating smoothed the original electroplated copper surface as shown by decrease of roughness Ra from 0.88 to 0.30 μm.

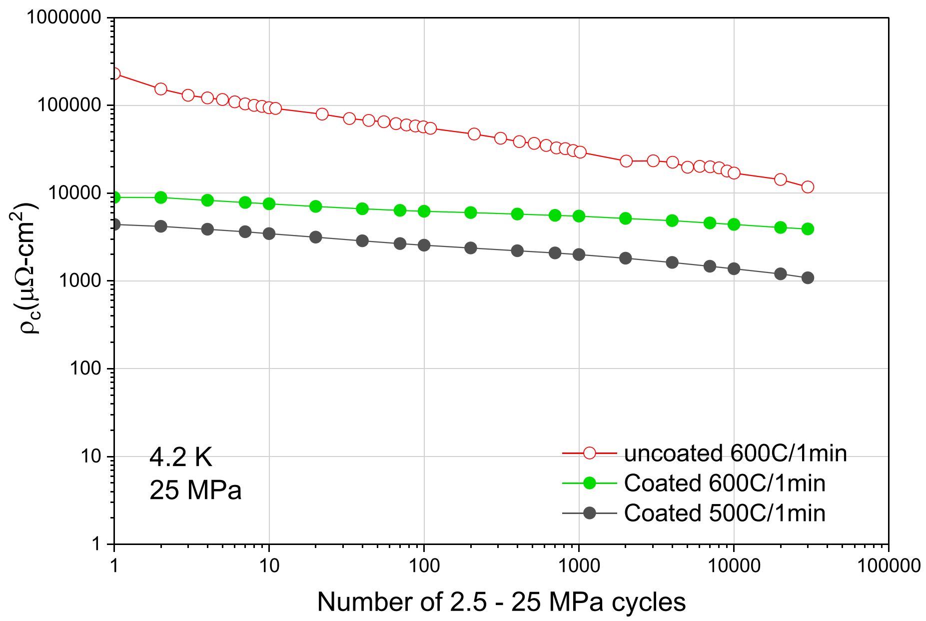

Figure 9. The effect coating solder on REBCO. ρ_c of REBCO/stainless steel/REBCO stack with solder-coated REBCO and an oxidized 25 μm thick stainless steel. Compared with non-coated case (data points of empty circle), initial ρ_c is reduced by more than one order of magnitude.

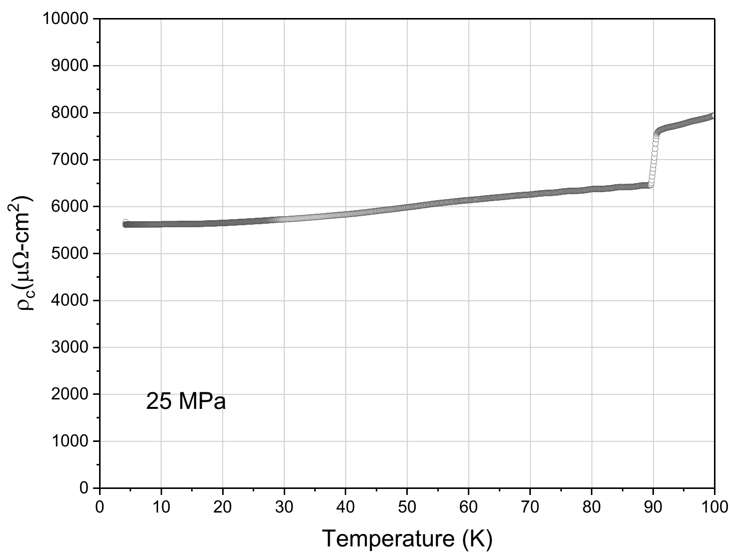

Figure 10. ρ_c versus temperature of a REBCO/stainless steel/REBCO. The stainless steel was in as-received condition with native oxide, silver epoxy (H20E) was applied between REBCO and stainless steel.

The solder coated REBCO were tested in REBCO/stainless steel/REBCO stacks (with no fillers). The results are shown in figure 9. Evidently, by coating REBCO with solder, ρ_c values were significantly lower than those shown in figure 3, and the load cycling effect is significantly reduced. These made the process suitable for our test coil, where ρ_c is to be controlled in the range of 1000–10 000 $\mu\Omega$-cm^2. This can be achieved by adjusting oxidation temperature of stainless steel co-wind tape in the range of 300 °C–600 °C.

It was previously reported that ρ_c between REBCO tapes is sensitive to temperature [7]. With oxidized stainless steel co-wind, however, the temperature dependence of REBCO/stainless steel/REBCO is dominated by the properties of the oxide and behaves differently. Figure 10 is the ρ_c temperature dependence measured under 25 MPa contact pressure, which shows that the temperature dependence is very weak. The implication of this result is that ρ_c at 77 K can represent the results at 4.2 K. This allowed us to do most of ρ_c control development at 77 K, which reduced costs and time considerably.

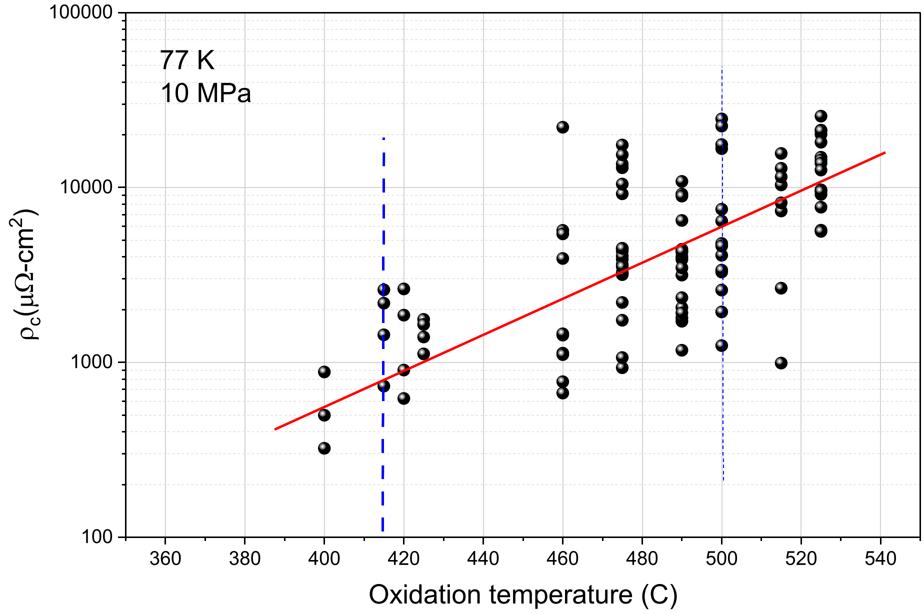

Figure 11. ρ_c of REBCO/stainless steel/REBCO at 77 K with 10 MPa contact pressure. REBCO samples were coated with solder, and the stainless steel were oxidized at different temperatures for 1 min. Due to the chimney effect of the vertical furnace, the actual temperature in the reel-to-reel oxidation system was not uniform and the maximum temperature which was at near the top of the furnace is typically 100 °C lower than the setpoints. The oxidation speed was about 1 m min^{-1}.

As a crucial step of the ρ_c control, we oxidized stainless steel tapes in reel-to-reel fashion at different temperatures and measured ρ_c of REBCO/stainless steel/REBCO, where the REBCO were solder coated. The oxidation temperature dependence of ρ_c at 77 K and 10 MPa is shown in figure 11. The ρ_c control development was aimed to be 1000 and 5000 $\mu\Omega$-cm^2 for test coils. Based on the results in figure 11, oxidation temperatures of 415 °C and 500 °C were chosen to achieve 1000 and 5000 $\mu\Omega$-cm^2 respectively. Their load cycling sensitivity was measured at 4.2 K as shown in figure 12(a), which is moderate and acceptable for future NI magnets. The corresponding ρ_c versus transverse pressure is shown in figure 12(b). ρ_c is shown to be insensitive to pressure.

3.3. Long length oxidized stainless steel tapes

To use this ρ_c control method described in section 3.2 in real magnet coils, it is necessary to ensure the consistency of ρ_c along the length. It is also necessary to measure ρ_c using the as-received stainless steel tapes because the thickness of native oxides on stainless steel surface is unknown and varies from batch to batch even by the same manufacturer. Figure 13 shows ρ_c of samples cut from a 17 m long stainless steel tape oxidized at 400 °C for 1 min. The average ρ_c value is 2000 $\mu\Omega$-cm^2 with a standard deviation of 388 $\mu\Omega$-cm^2, which is about 20% of the average value. Such a level of uncertainty must be considered in the quench calculation of NI coils.

For the PTC-6 test coil as described in the experimental section, developing ρ_c of the 1000 $\mu\Omega$-cm^2 was needed. Based on figures 11, 415 °C was chosen as the temperature for reel-to-reel oxidation. Subsequently, we measured ρ_c of multiple piece lengths of stainless steel tapes using the same pair of REBCO tapes. Furthermore, we developed ρ_c of the 5000 $\mu\Omega$-cm^2 for future NI coils of larger diameters. Both results are shown in figure 14. Of all the stainless steel tapes of 1.2 and 6.4 km targeted for 1000 and 5000 $\mu\Omega$-cm^2 respectively, the variation in ρ_c is on the order of 50%.

3.4. PTC-6 test coil

NI coil PTC-6 was fabricated and tested for major performance goals including ρ_c. The decay time constant after a sudden discharge at 5 A was measured; and ρ_c was calculated using equations (1) and (2). The results are tabulated in table 3 and plotted in figure 15.

As shown in table 3 and figure 15, ρ_c is in a range of 800–3000 $\mu\Omega$-cm^2. Two thermal cycles in event No. 4 were due to warming up the coil to room temperature for terminal repair. After the repair, the coil was cooled down to test in liquid nitrogen then warmed up followed by final cool down to 4.2 K. None of thermal cycling and the total of 1000 charge/discharge (210–100 A) cycles seems to change ρ_c significantly. This result demonstrates that our control of contact resistivity is successful in both

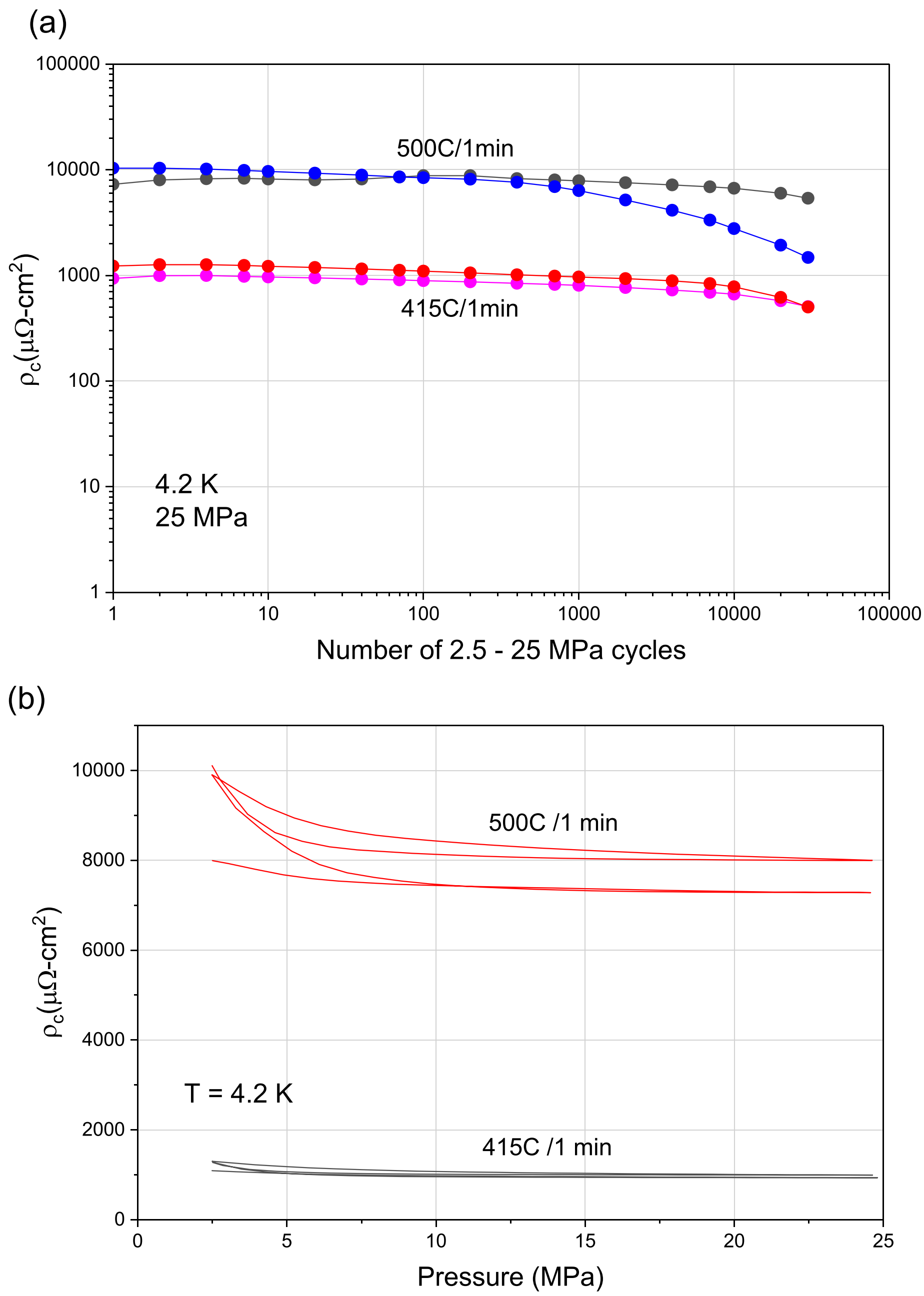

Figure 12. (a) ρ_c versus transverse load cycles targeting 1000 and 5000 $\mu\Omega$-cm^2. Two samples were measured for each oxidation condition. (b) ρ_c versus transverse pressure for two different heat treatments of stainless steel tapes.

achieving the designed ρ_c value and mitigation of load cycling sensitivity. Quenches induced by quench heaters, however, had significant impact on ρ_c, as shown at event 3, 6, and 7 in figure 15.

As can be seen in table 3, the PTC-6 coil was subjected to several forced quench. No spontaneous quenches occurred. There were no apparent signs of REBCO degradation; resistive voltages did not develop in the REBCO windings from the quenches, or cycling. After the test campaign, the double pancakes were unwound, and no evidence of overheating was found. Thus, the selection of target ρ_c appears to have been adequate for this coil size. The ρ_c is high enough that the stability level was sufficient to ramp the coil at 15 A/s (for the ramp cycles) and low enough to be sufficiently quench protected.

4. Discussions

Achieving reliable control of ρ_c is extremely challenging. It is unlikely that turn-to-turn contact resistance can be adjusted once the coil is wound. It must be tuned in the coil fabrication process by changing either the contact area [23], or ρ_c as in [24] and this work, or both [14, 25]. It also seems to

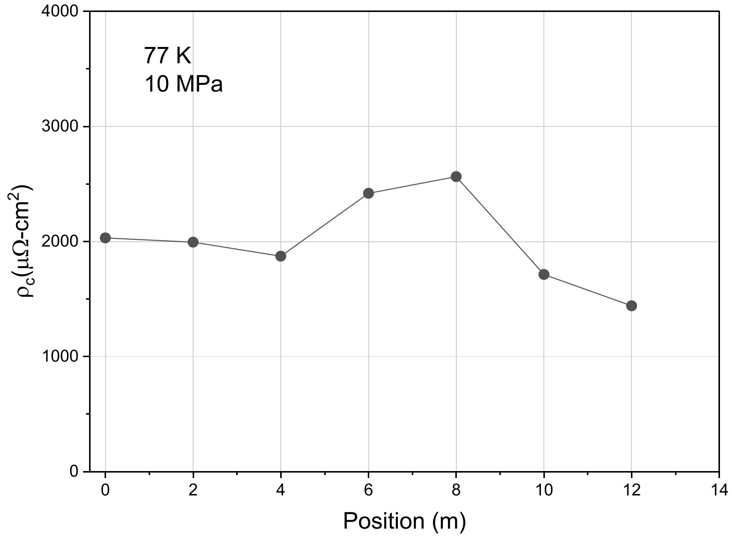

Figure 13. Variation of ρ_c along the length of stainless steel tape which was oxidized at 400 °C for 1 min. ρ_c was measured at 77 K under 10 MPa contact pressure. The same pair of solder coated REBCO were used for above tests.

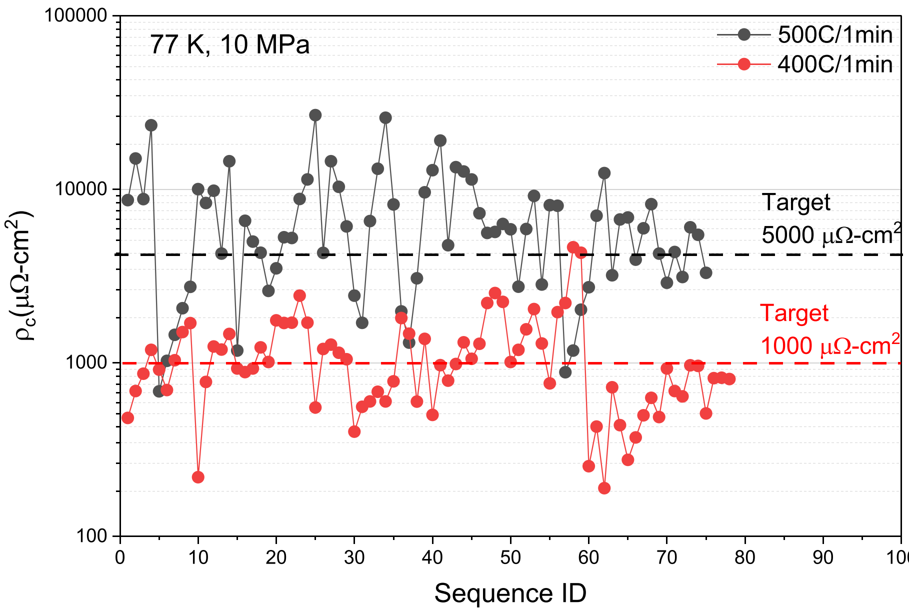

Figure 14. ρ_c measured with an oxidized stainless steel sandwiched between two solder-coated REBCO tapes targeting (a) 1000 $\mu\Omega$-cm^2 for use in PTC-6 and (b) 5000 $\mu\Omega$-cm^2.

be difficult to have a consistent ρ_c over a long length as figure 14 suggests. Similar variation in ρ_c among multiple double-pancakes was reported to be about 50% [16]. In addition, ρ_c varies with coil's radial stress, i.e. the contact pressure, which varies with radial position. Estimation of radial stress distribution is difficult due to large uncertainties in radial modulus of a dry-wound coil [26].

It is well known that real contacts are at asperities. Even with a seemingly perfect contact, the actual contact area is only a small fraction of the nominal contact area [27]. Since REBCO is vulnerable to further processing, the preferred way to control ρ_c is by deposition of a highly resistive thin film on the co-wind reinforcement tape. In this work, we showed that by combination of increasing contacting area with solder coating to decrease ρ_c and oxidation of stainless steel co-wind to increase ρ_c, the ρ_c can be adjusted in the range of 100–1000 000 $\mu\Omega\cdot$cm^2 with a relative uncertainty of about ± 50%. The considerable variation in ρ_c is understandable given that, with the variation in surface conditions of both REBCO and stainless steel, the actual contact area can vary significantly.

Table 3. ρ_c of PTC-6 by sudden discharge at 5 A and 4.2 K.

No.	Event	τ(s)	$R_c(\Omega)$	$\rho_c(\mu\Omega\text{-cm}^2)$
1	Before charging	0.533	0.1553	817
2	After HTS only 2 ramps to 240 A	0.473	0.1771	930
3	After 10 quench tests (one 240 A, nine 210 A)	0.239	0.3467	1821
4	After 2 thermal cycles	0.214	0.3840	2017
5	After 2 charging cycles to 230 A w/o LTS field	0.184	0.4475	2350
6	After 6 quench tests	0.141	0.5843	3069
7	After 7 more quench tests	0.274	0.3003	1577
8	After 500 cycles	0.266	0.3091	1624
9	After 500 cycles	0.301	0.2729	1434
10	At the end of coil test	0.261	0.3145	1652

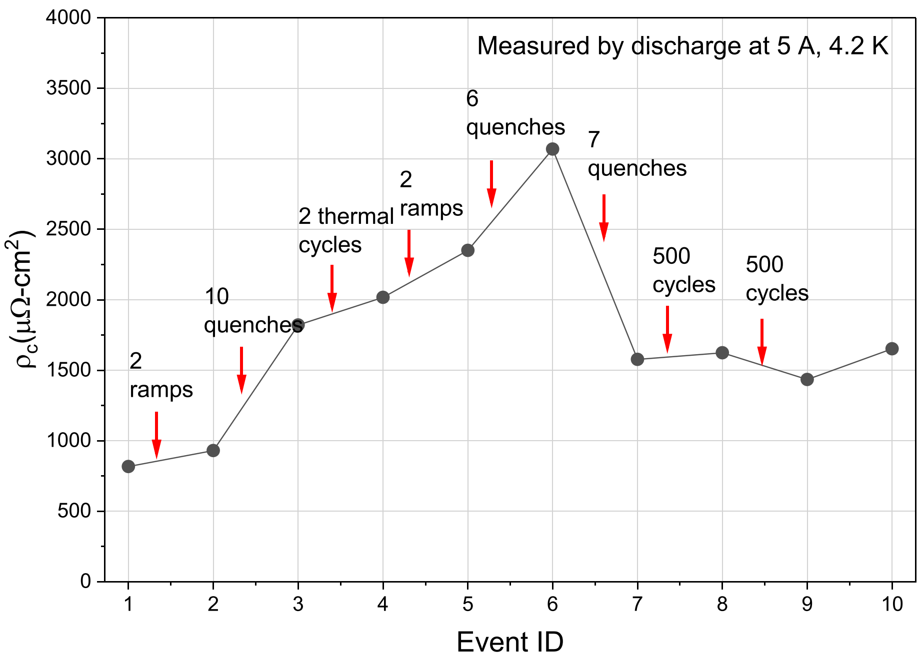

Figure 15. (a) PTC-6 ρ_c measured after a sequence of events as listed in table 3.

During testing of the NI coils, we found that the inductive voltage decayed to zero when a current ramp was held. The time-constant of this inductive voltage decay was comparable to the decay of central field Bz after a sudden discharge (figure 16(a)). This can be explained by the fact that inductive voltage is proportional to dBz/dt. When Bz had a charging delay due to contact resistance, dBz/dt behaved as what is shown in figure 16(b), which decays the same way as the inductive voltage. Figure 16(c) shows the current ramp and the Bz ramp with an apparent charging delay between 6.5 and 10 s. Therefore, the inductive voltage decay constant can be used for ρ_c measurement. It should be noted that, although inductive voltages were measured from each double-pancake, the decay time constants are all the same as they all correspond to dBz/dt. For nested coils with different designed ρ_c values, the measured time constant reflects an average of all the coils.

An important advantage of using inductive voltage method is that the measurement is done at the actual current and field conditions, so the effect of Lorentz stress on the contact is at the operating condition, whereas the sudden discharge tests are usually conducted at significantly lower current and fields to avoid coil damage. Chae *et al* [28] and Lee *et al* [29] used more elaborate simulation of inductive voltage during current ramps to obtain r_c. Due to the uncertainty introduced by the magnet current ramp rate, time constant values are prone to uncertainties. Sudden discharge method, on the other hand, results in more reproducible time constant values, and it usually generates large turn-to-turn current which is closer to the situation of a magnet quench. Therefore, it is a good method to study the impact of ρ_c on quench behavior and was used to generate data and presented in table 3 and figure 15. It is noteworthy that the apparent contact resistivity increase with increasing discharging current was observed by Liu *et al* [30].

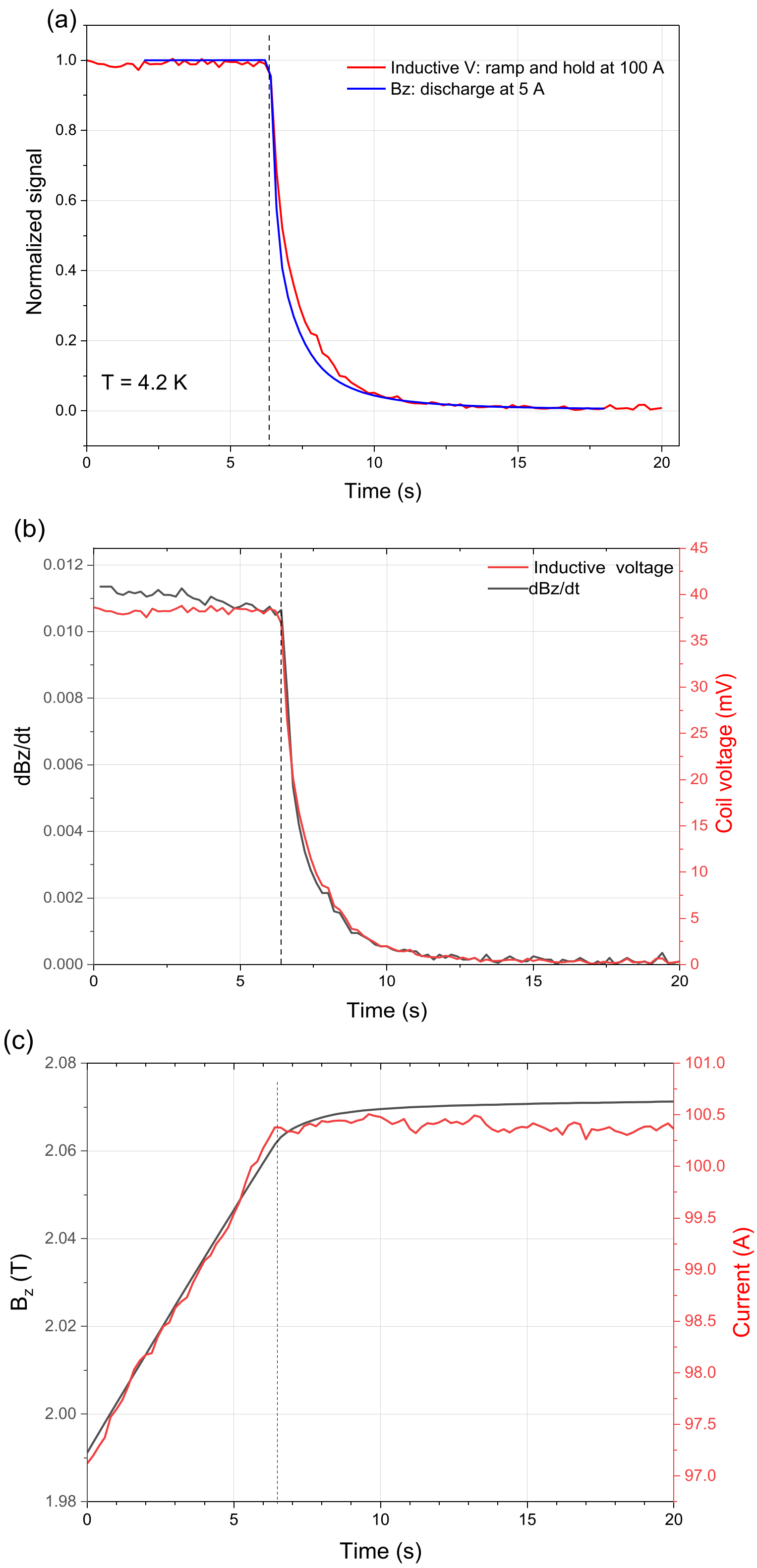

Figure 16. (a) Comparison between inductive voltage decay after a 0.5 A/s ramp and a field Bz decay after a sudden discharge from 5 A. (b) The inductive voltage decay versus dBz/dt. (c) Current and field ramp. The vertical dashed lines indicate the onset of the decays.

5. Conclusions

We developed a reliable method for controlling contact resistance ρ_c in NI REBCO coils. In our initial development efforts, we demonstrated ρ_c control by oxidation of stainless steel co-wind tapes. To mitigate the load cycling effect on ρ_c, silver paste and silver epoxy were applied at the interface between

REBCO and stainless steel. While this wet winding method has its merit, it raises the concern that the epoxy may result in REBCO delamination. We found that in dry-wound coil the loading cycling effect is minimized by coating REBCO with a thin layer of PbSn solder. Both oxidation of stainless steel co-wind tapes and solder coating of REBCO tapes were done in a reel-to-reel fashion for long length application. REBCO and stainless steel tapes treated by these methods were used in a six double-pancake test coil. The coil test results showed that the average ρ_c of the coil was in good agreement with the designed value of 1000 $\mu\Omega$-cm^2. A method of measuring coil's ρ_c by the decay time of coil's inductive voltage is proposed.

Acknowledgment

We thank Dr Eric Lochner for helping with atomic-layer-deposition of TiN and Al_2O_3 on stainless steel samples, Robert Goddard for confocal laser microscopy measurements, and Professor Seungyong Hahn for providing the program for ρ_c calculation. This work was performed at the National High Magnetic Field Laboratory, which is supported by National Science Foundation Cooperative Agreement Nos. DMR-2131790 and DMR-2128556, and the State of Florida.

Data availability statement

All data that support the findings of this study are included within the article (and any supplementary files).

ORCID iDs

Jun Lu 0000-0001-8521-489X
Denis Markiewicz 0000-0002-6888-0150
Hongyu Bai 0000-0002-3834-1615
Mark Bird 0000-0001-9617-2875

References

[1] Hahn S *et al* 2019 45.5-tesla direct-current magnetic field generated with a high-temperature superconducting magnet *Nature* **570** 496–9
[2] Liu J *et al* 2020 World record 32.35 tesla direct-current magnetic field generated with an all-superconducting magnet *Supercond. Sci. Technol.* **33** 03LT01
[3] Zhang X *et al* 2024 Strain analysis and preliminary test of an all-superconducting high-field magnet generating 32.4 T direct-current magnetic field *Supercond. Sci. Technol.* **37** 125003
[4] Suetomi Y *et al* 2021 Quench and self-protecting behaviour of an intra-layer no-insulation (LNI) REBCO coil at 31.4 T *Supercond. Sci. Technol.* **34** 064003
[5] Fazilleau P, Chaud X, Debray F, Lécrevisse T and Song J-B 2020 38 mm diameter cold bore metal-as-insulation HTS insert reached 32.5 T in a background magnetic field generated by resistive magnet *Cryogenics* **106** 103053
[6] Markiewicz W D, Painter T, Dixon I and Bird M 2019 Quench transient current and quench propagation limit in pancake wound REBCO coils as a function of contact resistance, critical current, and coil size *Supercond. Sci. Technol.* **32** 105010
[7] Lu J, Xin Y, Lochner E, Radcliff K and Levitan J 2020 Contact resistivity due to oxide layers between two REBCO tapes *Supercond. Sci. Technol.* **33** 045001
[8] Xue S, Sumption M D, Panik D, Thong C J, Guo X, Majoros M and Collings E W 2022 Electrical contact resistance in REBCO stacks and cables with modified surfaces *IEEE Trans. Appl. Supercond.* **32** 4802506
[9] Genot C, Lécrevisse T, Fazilleau P and Tixador P 2023 Experimental measurements of contact resistivity between superconducting HTS tapes with or without metallic co-wound tape *Cryogenics* **132** 103691
[10] Lécrevisse T, Chaud X, Fazilleau P, Genot C and Song J-B 2022 Metal-as-insulation HTS coils *Supercond. Sci. Technol.* **35** 074004
[11] Lee L, Lee J, Mun J, Kim J, Sim K, Hahn S and Kim S 2022 A study on the electrical contact resistance and thermal conductivity of soldered-metal insulation coil with conduction cooling *IEEE Trans. Appl. Supercond.* **32** 4604805
[12] Lu J, Dixon I, Kim K, Deterding J, Marks L, Jarvis B, Markiewicz W D, Bai H and Bird M2023 Control of turn-to-turn contact resistivity for resistive insulated REBCO coils 1OrA1-7 *MT28 Int. Conf. on Magnet Technology* (*Aix-on-Provence, France, 10–15 September, 2023*)
[13] Bouloukakis K, Hunter M, Long N and Dykstra R 2021 Discharge behaviour and modelling of a 1.5 T REBCO magnet with quench tolerant coils impregnated with conductive epoxy *IEEE Trans. Appl. Supercond.* **31** 4601105
[14] Seo J *et al* 2025 Application of electrically-conductive epoxy in no-Insulation coils for controlling contact resistance *IEEE Trans. Appl. Supercond.* **35** 470190
[15] Weijers H W *et al* 2014 Progress in the development of a superconducting 32 T magnet with REBCO high field coils *IEEE Trans. Appl. Supercond.* **24** 4301805
[16] Fazilleau P, Borgnic B, Chaud X, Debray F, Lécrevisse T and Song J-B 2018 Metal-as-insulation sub-scale prototype tests under a high background magnetic field *Supercond. Sci. Technol.* **31** 095003

[17] Lu J, Goddard R, Han K and Hahn S 2017 Contact resistance between two REBCO tapes under load and load cycles *Supercond. Sci. Technol.* **30** 045005

[18] Ultra Blak 407 Safety data sheet, EPI 2022 (available at: www.epi.com/amfile/file/download/file/1746/product/1152/)

[19] Park S *et al* 2024 Contact resistance and over-current characteristics of no-Insulation high-temperature superconducting coils impregnated with an electrically conductive epoxy *IEEE Trans. Appl. Supercond.* **34** 6601705

[20] Takematsu T, Hua R, Takao T, Yanagisawa Y, Nakagome H, Uglietti D, Kiyoshi T, Takahashi M and Maeda H 2010 Degradation of the performance of a YBCO-coated conductor double pancake coil due to epoxy impregnation *Physica C* **470** 674–7

[21] Online Materials Information Resource - MatWeb (available at: www.matweb.com/)

[22] R A Chilton Properties of Electroplated Copper (available at: www.rachilton.com/copperproperties.html)

[23] Slade R, Kruip M, van Nugteren B, Brittles G, de Villa Valdés E R, Bateman R and Down A 2020 Partially Insulated HTS coils', patent, US 2020/0365304 A1

[24] Zhang Z, Wang L, Zhang H, Suo H, Liu J and Wang Q 2024 'The possible control method of turn-to-turn contact resistivity of REBCO coil by surface coating *IEEE Trans. Appl. Supercond.* **34** 4601805

[25] Kawahata M, Tanaka Y, Suetomi Y, Imanishi S, Nakamura K, Takao T, Piao R, Kobayashi K, Yamazaki T and Yanagisawa Y 2025 Resistance-controlled (RC) interface with metal mesh for managing current bypassing in no-insulation (NI) scheme coils *IEEE Trans. Appl. Supercond.* **35** 470220

[26] Yan Y, Kim J, Bong U, Jang W, Kim G, Park J and Hahn S 2023 Measurement and analysis of winding stresses in dry-wound pancake coils considering nonlinear compressive behaviors *Supercond. Sci. Technol.* **36** 115019

[27] Slade P G 2013 *Electrical Contacts, Principles and Applications* 2nd edn (CRC Press)

[28] Chae Y S, Kim J H, Quach H L, Lee S H and Kim H M 2021 Analysis on electrical and thermal characteristics of MI-SS racetrack coil under conduction cooling and external magnetic field *Prog. Supercond. Cryog.* **23** 61–9

[29] Lee J T, Kim G, Kim J, Bang J, Im C, Jang W, Choi K, Yoon M, Kim W-S and Hahn S 2023 Experimental and equivalent circuit analysis approach to estimate contact resistances on different sections in a D-shaped NI HTS coil *IEEE Trans. Appl. Supercond.* **33** 4603205

[30] Liu S, Wang L, Zhang Z, Wang L, Zhou B, Chen Y, Wang L and Wang Q 2024 Exploration of the influence factors on contact resistance obtained from sudden discharge test on the large-bore metal-as-insulation REBCO magnet *Supercond. Sci. Technol.* **37** 115017